Structure beyond Bragg: Study of V_2O_5 nanotubes

V. Petkov,[1,*] P. Y. Zavalij,[2] S. Lutta,[2] M. S. Whittingham,[2] V. Parvanov,[1] and S. Shastri[3]
[1]*Department of Physics, Central Michigan University, Mt. Pleasant, Michigan 48859, USA*
[2]*Chemistry Department, State University of New York at Binghamton, Binghamton, New York 13902, USA*
[3]*Advanced Photon Source, Argonne National Laboratory, Argonne, Illinois 60439, USA*
(Received 5 November 2003; published 25 February 2004)

The structure of V_2O_5 nanotubes has been experimentally determined. The approach of the atomic pair distribution function technique was employed because of the limited structural coherence in this nanophase material. It has been found that even a nanocrystal with the complex morphology of vanadium pentoxide nanotubes possesses an atomic arrangement very well defined on the nanometer length scale and well described in terms of a unit cell and symmetry. Using refined structural parameters a real-size model for the nanotubes has been constructed and used to explain their peculiar morphology.

DOI: 10.1103/PhysRevB.69.085410 PACS number(s): 73.63.Fg, 61.46.+w, 61.43.−j

I. INTRODUCTION

Knowledge of the atomic-scale structure is an important prerequisite to understand and control the properties of materials. In the case of crystals it is obtained solely from the Bragg peaks in their diffraction pattern and is given in terms of a small number of atoms placed in a unit cell subjected to symmetry constraints. However, many materials of technological importance, including nanophase materials, do not possess the long-range order of conventional crystals and often it is this deviation from perfect order that makes them technologically and/or scientifically important. An important example is vanadium pentoxide. Crystalline vanadium pentoxide, V_2O_5, is a key technological material widely used in applications such as optical switches, chemical sensors, catalysts, and solid-state batteries.[1–5] The material possesses an outstanding structural versatility and can be manufactured into nanotubes that have many of the useful physicochemical properties of the parent V_2O_5 crystal significantly enhanced. For example, the high specific surface area of the nanotubes renders them even more attractive as positive electrodes in secondary Li batteries.[6] Also, the nanotubes show significantly increased capability for redox reactions.[7,8] In addition, the nanostructured material shows a good potential for completely novel applications such as nanoactuators[9] and nonlinear optical limiters.[10] The synthetic route employed in the preparation of the nanotubes involves a sol-gel reaction and uses organic molecules as structure directing agents.[11–13] The tubes produced are up to 15 μm long and have inner diameters between 5 and 15 nm while the outer diameters range from 15 to 100 nm. Their walls consist of several vanadium oxide layers with the organic molecules intercalated in between them as can be seen in Fig. 1. Transmission electron microscopy (TEM) images of even higher resolution[11,12] reveal that V_2O_5 nanotubes are indeed with serpentinelike morphology and exist as either scrolls or closed cylinders. The diffraction pattern of a material with such a complex morphology and limited structural coherence shows a pronounced diffuse component and only a few Bragg peaks (see Fig. 2). This limits the applicability of traditional techniques for structure determination. Here we show that the challenge can be met by employing a nontraditional experimental approach going beyond Bragg scattering in the diffraction data. The approach is that of the atomic pair distribution function technique (PDF). It takes both the diffuse and Bragg components of the diffraction data into account and yields atomic ordering in terms of quantitative parameters such as a unit cell and symmetry even when the material is ordered only on the nanometer length scale as is the case with vanadium pentoxide nanotubes.

II. EXPERIMENT

A. Sample preparation

Vanadium oxide nanotubes were synthesized following the method introduced by Reinoso *et al.*[14] with slight modifications. A mixture of vanadium (V) oxide and dodecylamine in equamolar ratio in absolute ethanol (3 ml/g of V oxide) was stirred in air for 2 h and then hydrolysized with osmosis reversed water (5 ml/g of V oxide). After aging for 3 days and hydrothermal treatment in an autoclave at 180 °C for 7 days, a black precipitate was obtained. The product was washed with water, ethanol, hexane, and diethyl ether (3 $\times$50 ml each) to remove the unreacted amines and decomposed products, and dried overnight under vacuum at 80 °C to prevent oxidation of vanadium 4+ to 5+. Thus prepared powder was sealed between Kapton foils and subjected to x-ray diffraction (XRD) experiments.

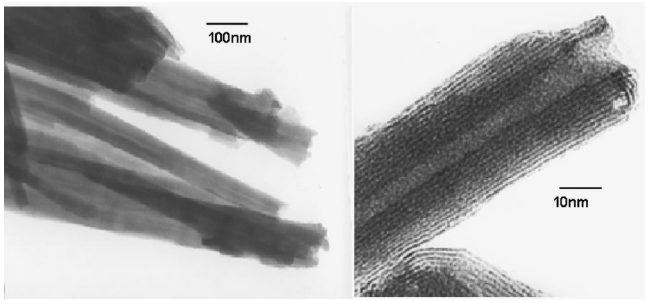

FIG. 1. TEM images of vanadium oxide nanotubes used in the present study; wrapping layers can be seen at higher magnification (right).

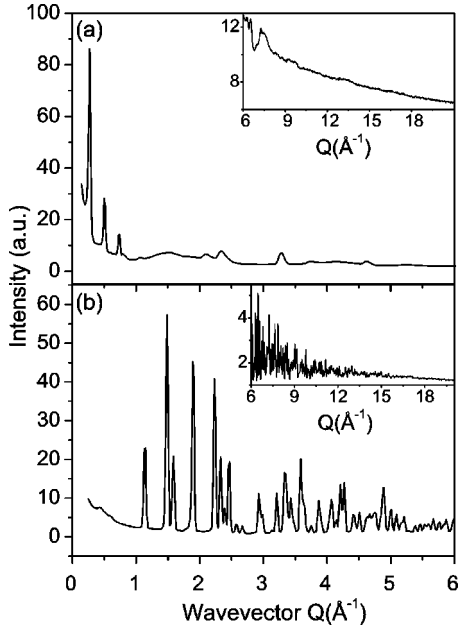

FIG. 2. Experimental powder diffraction patterns for V_2O_5 nanotubes (a) and crystalline V_2O_5 (b). The high-Q portion of the patterns is given in the insets on an enlarged scale.

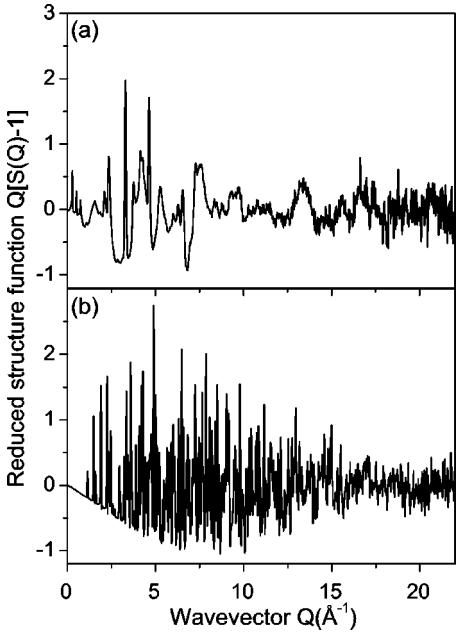

FIG. 3. Experimental structure functions for V_2O_5 nanotubes (a) and crystalline V_2O_5 (b) extracted from the diffraction data of Fig. 2.

B. X-ray diffraction experiments

The diffraction experiments were carried out at the 1-ID beam line at the Advanced Photon Source (APS), Argonne National laboratory. The measurements were done in symmetric transmission geometry at room temperature using x rays of energy 80.6 keV. The use of x rays of such a high energy allows one to access higher wave vectors which is essential for obtaining PDF's of good real-space resolution. Also, it helps reduce several unwanted experimental effects such as absorption and multiple scattering. Several runs were conducted and the resulting XRD patterns were averaged to improve the statistical accuracy and to reduce any systematic effect due to instabilities in the experimental setup. Thus obtained XRD patterns for vanadium oxide nanotubes and crystalline V_2O_5 are shown in Fig. 2. Only the elastically scattered intensities $I^{\mathrm{el}}Q$ were extracted from the raw diffraction data and the so-called structure functions $S(Q)$,

$$S(Q)=1+\left[I^{\mathrm{el}}(Q)-\sum c_i\left|f_i(Q)\right|^2\right]\Big/\left|\sum c_i f_i(Q)\right|^2, \tag{1}$$

were derived, where c_i and $f_i(Q)$ are the atomic concentration and x-ray scattering factor, respectively, for the atomic species of type i (Ref. 15). Then the corresponding reduced atomic pair distribution function $G(r)$ was calculated via a Fourier transformation as follows:

$$G(r)=(2/\pi)\int_{Q=0}^{Q_{\max}} Q[S(Q)-1]\sin(Qr)dQ. \tag{2}$$

Here Q is the magnitude of the wave vector ($Q=4\pi\sin\theta/\lambda$), 2θ is the angle between the incoming and outgoing radiation, and λ is the wavelength of the radiation used. By definition the atomic PDF $G(r)$ gives the deviation of the local $\rho(r)$ from the average ρ_0 atomic number density:

$$G(r)=4\pi r[\rho(r)-\rho_0]. \tag{3}$$

It peaks at real-space distances where the local atomic number density $\rho(r)$ exceeds the average one—i.e., where most frequent atomic pair distances occur—and thus reflects the atomic-scale structure of materials. Thus obtained experimental structure functions $S(Q)$ and PDFs $G(r)$ are shown in Figs. 3 and 4, respectively. All calculations were done with the help of the program RAD (Ref. 16).

III. RESULTS AND DISCUSSION

As can be seen in Fig. 2 the lack of perfect long-range order due to the curvature of the tube walls has a profound effect on the diffraction pattern of nanophase V_2O_5. While the diffraction pattern of crystalline vanadium pentoxide shows sharp Bragg peaks up to wave vectors as high as $Q\sim 15$ Å^{-1} that of the nanotube counterpart shows only a few Bragg-like features that merge into a slowly oscillating diffuse component already at Q values of approximately 6–8 Å^{-1}. The Bragg-like features in the diffraction pattern of the nanotubes can be subdivided into two groups. The first one includes three relatively sharp peaks seen at wave vectors shorter than 1 Å^{-1} [see Fig. 2(a)]. Those peaks reflect the spacing ($\approx$20 Å) between the individual vanadium oxide layers building the walls of the nanotubes and shift anytime a different organic molecule is used as a structure directing template. The second group includes all higher-Q peaks which, contrary to the lower-Q ones, do not change their position with the change of the organic template and, therefore, may be associated with the atomic ordering within the vanadium oxide layers. This group of peaks can be indexed

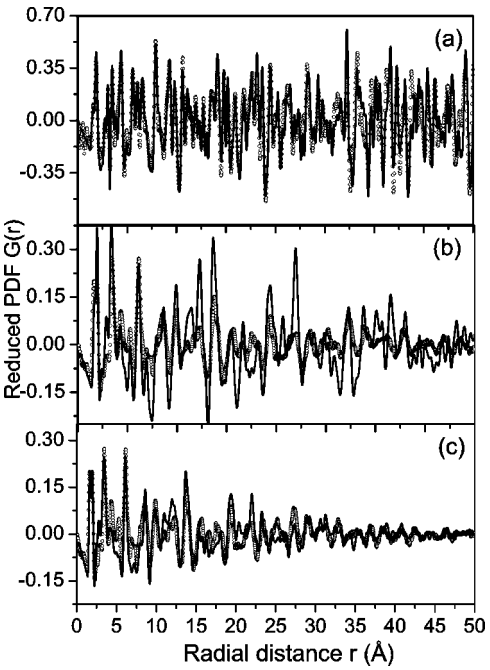

FIG. 4. Comparison between experimental (circles) and model (solid line) PDF's for (a) crystalline V_2O_5 and its well-known orthorhombic structure (Ref. 20), (b) V_2O_5 nanotubes and the triclinic $BaV_7O_{16}\cdot nH_2O$-type structure (Ref. 24), and (c) V_2O_5 nanotubes and a structure refined against the experimental PDF data. The refined structural parameters for vanadium oxide nanotubes are given in Table I.

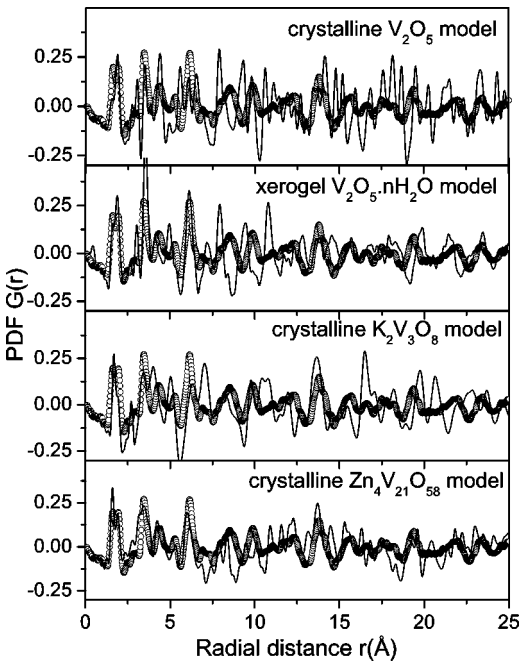

FIG. 5. Comparison between the experimental PDF for V_2O_5 nanotubes (circles) and model PDF's (solid line) for vanadium oxides with the structures shown in Fig. 6. The model data show the best fit to the experimental data that was possible to be achieved within the symmetry constraints of the respective structures.

in a two-dimensional tetragonal cell with $a=6.16$ Å. The finding reveals the presence of a well-defined structural unit that builds the nanotube walls in a repetitive manner. Remarkably, regardless of the differences in the preparation routes employed, all varieties of V_2O_5 nanotubes manufactured so far are found to exhibit very similar diffraction patterns, indicating that they all share a similar atomic arrangement, including the repetitive structural unit. The limited number of Bragg peaks, however, makes it impossible to apply traditional techniques for structure determination such as Rietveld refinement[17] and reveal the unit in detail. One solution to the problem is to apply a nontraditional approach such as the atomic PDF technique that is capable of handling diffraction patterns of the type shown in Fig. 2(a). We already demonstrated that the approach works well with bulk nanocrystals such as $LiMoS_2$ and $V_2O_5\cdot nH_2O$ nanoribbons.[18,19] Now we show that it also can be successfully applied to nanocrystals with a much more complex, tubular morphology.

The approach is as follows: Bragg-like features in the diffraction pattern of the nanocrystalline material are carefully considered to identify the presence of an approximate repetitive structural unit and find its parameters and symmetry, if possible. Plausible structural models that are consistent with the unit cell as well as with all available structural information for the material under study are looked for. Usually such models are not difficult to find among the crystalline counterparts of the nanomaterial or to be constructed by first-principles (Ref. 18 and references therein) or semi-empirical calculations. Then, like all powder-diffraction techniques, the three-dimensional structure is determined through matching and refining the models against the experimental diffraction data. Since, as exemplified in Fig. 2(a), the number of Bragg peaks is limited, the diffraction data are first reduced to the so-called structure function $Q[S(Q)-1]$ [see Eq. (1)] and then Fourier transformed [see Eq. (2)] to the corresponding atomic PDF. This experimentally derived PDF is indeed the quantity that guides the structure determination process. A comparison between the data in Figs. 2, 3, and 4 demonstrates the importance of this step. As Fig. 2 shows the diffraction data are usually dominated by strong Bragg features at lower Q values and, in this form, are mainly sensitive to the long-range atomic ordering in materials. In the corresponding structure functions $Q[S(Q)-1]$ all diffraction features, including those at higher wave vectors, appear equally strong (see Fig. 3) and are thus of equal importance in structure determination. This enhances the sensitivity to local atomic ordering and makes the Fourier couple $Q[S(Q)-1]$/PDF an experimental quantity that is very well suited to study the structure of materials with limited structural coherence. That V_2O_5 nanotubes are such a material is clearly seen in Fig. 4 showing the experimental PDF decaying to zero already at 50 Å. In contrast, the PDF of crystalline V_2O_5 persists to very long real-space distances as it should be with a material exhibiting a long-range order. In either case the atomic PDF is rich in well-defined, structure-sensitive features reflecting the relative positions of atoms. This is well demonstrated in Fig. 4(a) where a model PDF based on the well-known structure of crystalline V_2O_5 (Ref. 20) is compared to the experimental PDF. The agree-

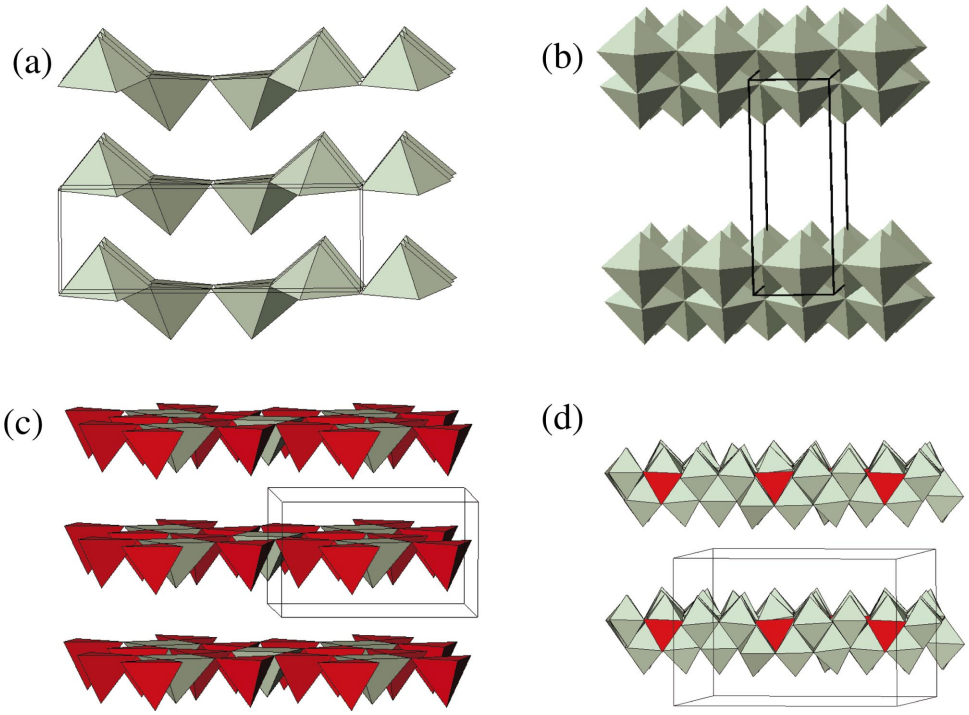

FIG. 6. (Color) Fragments of the structures of various vanadium oxides: (a) V_2O_5 crystal, (b) $V_2O_5 \cdot nH_2O$ gel, (c) $K_2V_3O_8$, and (d) $Zn_4V_{21}O_{58}$. For the sake of clarity only structural units involving vanadium and oxygen atoms are shown: square pyramidal V-O_5 and distorted octahedral V-O_6 units are in light green and tetrahedral V-O_4 units are in red, respectively. The corresponding unit cells are shown as thin lines.

ment between model and experimental data is very good and well documents the fact that atomic PDF's can provide a reliable basis for structure determination.

A comparison between the experimental PDF's for V_2O_5 crystals and nanotubes shows (see Figs. 4 and 5) that both exhibit an almost split-up first peak positioned between 1.6 Å and 2.0 Å. The peak reflects the immediate coordination of vanadium atoms which, in the crystal, involves four equato-

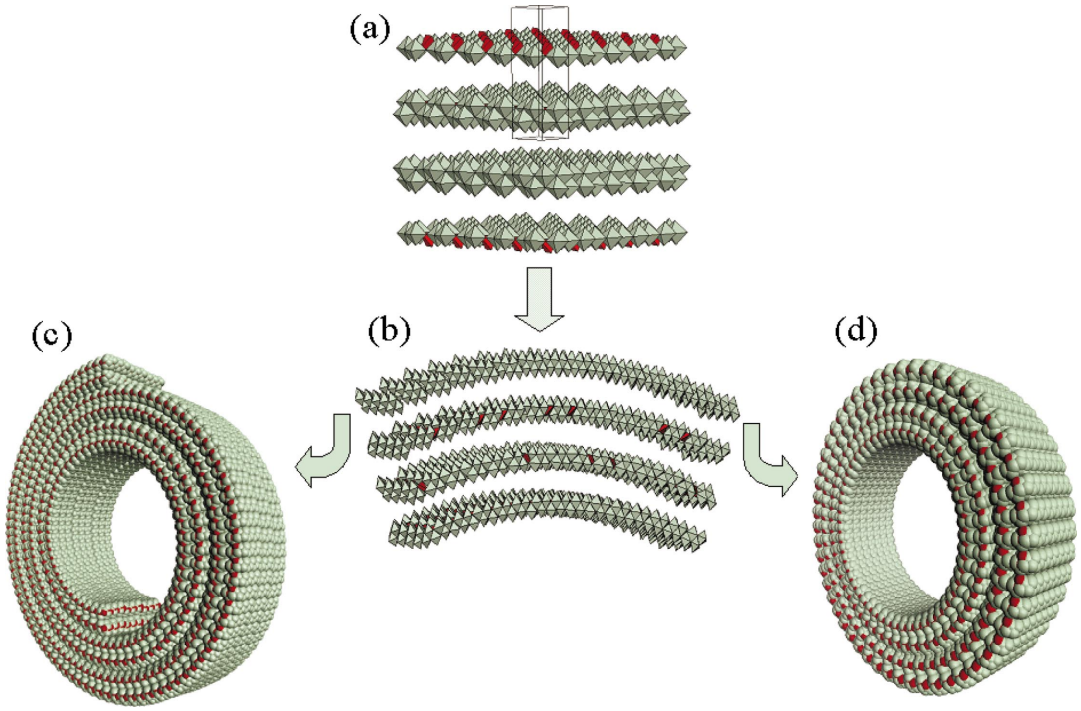

FIG. 7. (Color) Structure description of V_2O_5 nanotubes. Double layers of V-O_6 octahedral (light green) and V-O_4 tetrahedral (red) units are undistorted and stacked in perfect registry with crystalline $BaV_7O_{16} \cdot nH_2O$ (a). When bent (b) such layers may form nanoscrolls (c) or closed nanotubes (d). Double layers of such complexity may sustain only a limited deformation. As a result, V_2O_5 nanotubes occur with inner diameters not less than 5 nm. The real-size models shown in (c) and (d) have an inner diameter of approximately 10 nm and involve 33 000 atoms. The bending of vanadium oxide layers into nanotubes can be explained by the presence of an anisotropy in the distribution of vanadium 4+ and 5+ ions as discussed in Ref. 24.

rial oxygens at 1.8–2 Å and an axial oxygen at ~1.6 Å arranged on the vertices of a square pyramidal unit. If a more distant oxygen at ~2.4 Å is also considered, the oxygen coordination of vanadium becomes a distorted octahedron. Although the immediate V-O coordination in both the crystal and nanomaterial appears similar, the spatial arrangement of V-O polyhedra in them is quite different as reflected by the very different behavior of the corresponding atomic PDF's at longer real-space distances (see Fig. 4). To determine the atomic arrangement in the nanotubes we explored several models based on structures occurring with crystalline vanadium oxides exhibiting various arrangements of V-O polyhedra. The basic structural units of the models were adjusted to approach as close as possible the size of the repetitive structural unit ($\sim 6\ \text{Å} \times 6\ \text{Å} \times 20\ \text{Å}$) observed with the nanotubes. The coordinates of the atoms inside the unit cells were also adjusted accordingly. Then these structural parameters (unit cell and atomic coordinates) were varied so as to obtain the best possible agreement between the calculated and experimental PDF data while strictly observing the constraints imposed by the respective local symmetry. The calculations were done with the help of the program PDFFIT (Ref. 21). At first, a model based on the 14-atom unit cell of crystalline V_2O_5 (Ref. 20) was attempted. As can be seen in Fig. 5 the model does not reproduce the experimental data well especially in the region beyond the first PDF peak. This shows that V_2O_5 nanotubes may not be considered as built of single layers of square pyramidal V-O_5 units that occur in crystalline V_2O_5 [see Fig. 6(a)]. Since the nanotubes were obtained via a sol-gel route, a model based on the structure of $V_2O_5 \cdot nH_2O$ gel[19] was tested as well. That model also failed to reproduce the experimental data as can be seen in Fig. 5. The unsuccessful outcome showed that V_2O_5 nanotubes are not built of double layers of square pyramidal/octahedral V-O_5 units that occur in $V_2O_5 \cdot nH_2O$ gel [see Fig. 6(b)].

Then we turned our attention to models allowing two types of vanadium-oxygen coordination: tetrahedral V-O_4 and square pyramidal V-O_5. The presence of V-O_4 units in the nanotubes was prompted by findings of previous magnetic susceptibility and x-ray photoelectron spectroscopy experiments.[11] As trial structures we used that of $K_2V_3O_8$ (Ref. 22) and $Zn_4V_{21}O_{58}$ (Ref. 23) featuring single [see Fig. 6(c)] and double [see Fig. 6(d)] layers of vanadium-oxygen tetrahedra and pyramids/octahedra, respectively. For the sake of simplicity we considered only vanadium and oxygen atoms in our model calculations shown in Fig. 5. As can be seen in the figure those two models reproduce the main features in the experimental PDF data better than the ones featuring a single type of V-O units but still fail in some important details, such as, for example, the shape of the first PDF peak.

Finally, we approached the atomic ordering in the nanotubes by considering that found in crystalline $BaV_7O_{16} \cdot nH_2O$ which may be viewed as an ordered assembly of double layers of pyramidal/octahedral vanadium-oxygen units with a small number of V-O_4 tetrahedra embedded into the layers [see Fig. 7(a)]. The peculiar atomic ordering of $BaV_7O_{16} \cdot nH_2O$ and its relevance to vanadium pentoxide nanotubes has already drawn some attention.[11,12,24] The stacking of the layers in $BaV_7O_{16} \cdot nH_2O$ occurs in two modifications: triclinic[24] and tetragonal.[25] From the two modifications only the triclinic one showed good promise in the PDF fitting process. A model PDF based on that modification is shown on Fig. 4(b). Again only vanadium and oxygen atoms were considered in the model calculations. This model was an excellent starting point and could be refined to reproduce very well all important details in the experimental data as shown in Fig. 4(c). The refined structural parameters are summarized in Table I. The agreement with the PDF data is somewhat worse than that achieved with crystalline V_2O_5 [compare Figs. 4(a) and 4(c)]; however, given the high degree of disorder inherent in the nanotubes this level of agreement is quite good and acceptable.

TABLE I. Parameters of the basic structural unit and coordinates of the atoms in it for V_2O_5 nanotubes as determined by the present PDF study. $a = 6.020(3)$ Å, $b = 6.1305(25)$ Å, $c = 18.973(10)$ Å, $\alpha = 93.2351(9)°$, $\beta = 91.0673(9)°$, $\gamma = 90.0675(9)°$; S.G. $P\bar{1}$.

Atom	x/a[a]	y/b	z/c
V(1)	0.906	0.534	0.330
V(2)	0.372	0.360	0.323
V(3)	0.657	0.450	0.181
V(4)	0.528	0.781	0.328
V(5)	0.933	0.007	0.252
V(6)	0.205	0.592	0.158
V(7)	0.438	0.973	0.168
O(1)	0.438	0.061	0.304
O(2)	0.234	0.646	0.306
O(3)	0.925	0.516	0.198
O(4)	0.409	0.237	0.190
O(5)	0.694	0.134	0.203
O(6)	0.617	0.455	0.308
O(7)	0.358	0.371	0.411
O(8)	0.387	0.024	0.067
O(9)	0.804	0.848	0.316
O(10)	0.045	0.241	0.308
O(11)	0.468	0.717	0.175
O(12)	0.896	0.572	0.414
O(13)	0.140	0.984	0.184
O(14)	0.115	0.575	0.080
O(15)	0.663	0.411	0.088
O(16)	0.511	0.801	0.411

[a]The uncertainty in the atomic coordinates is ±0.002.

The outcomes of the structure determination unambiguously show that even a nanocrystal with the complex morphology of vanadium pentoxide nanotubes possesses an atomic-scale structure very well defined on the nanometer length scale and well described in terms of a unit cell and symmetry. The unit cell is of triclinic $P\bar{1}$ symmetry, with dimensions of approximately $6 \times 6 \times 19\ \text{Å}^3$ and contains only 46 atoms arranged in a pattern very similar to that observed with crystalline $BaV_7O_{16} \cdot nH_2O$.

As we demonstrated in a study of nanocrystalline $LiMoS_2$,[18] atomic coordinates obtained by the PDF tech-

nique can be used to calculate structure-dependent characteristics of nanostructured materials such as electronic band structure with success. Now we make the next step and show that knowing the repetitive structural unit of a nanocrystal allows us to construct real-size models that again can be used to predict and understand material's properties. A real-size model of V_2O_5 nanotubes was constructed by mapping the unit cell determined by the PDF technique onto a cylindrical surface as shown in Fig. 7. Care was taken not to destroy the integrity and local symmetry of the individual vanadium-oxygen layers since the diffraction experiments show them well preserved in the nanomaterial. It turned out that this could only be achieved when the diameters of the model nanotubes were of the order of 5 nm or larger. It appears then that the complexity of the atomic-scale structure plays an important role in determining the morphology of the nanocrystals. Carbon nanotubes are built of graphitic sheets one atomic layer thin that are flexible enough to bend into tubes of diameter of 1 nm or so.[26] Vanadium oxide nanotubes are built of layers of much more complex structure (see Fig. 7) that can only be accommodated in nanotubes of diameters of 5 nm or larger.

IV. CONCLUSION

In summary, the atomic-scale structure of nanocrystals can be determined in terms of a small number of structural parameters by employing a nontraditional approach such as the atomic PDF technique allows. The technique relies on diffraction data obtained from the nanomaterial: it is sensitive to fine structural features including the immediate atomic ordering and could easily differentiate between competing structural models (see Figs. 5 and 6). Once a good structural model is found its parameters (unit cell and atomic coordinates) may be refined [see Figs. 4(b) and 4(c)] and then used to explain, predict, and possibly improve the structure-sensitive properties of the material. This is a major advantage over the traditional crystallographic techniques that may identify but may not refine the structural characteristics of a nanocrystal. Also, this is a major advantage over employing a statistical description of the structure as it is done with completely disordered materials such as glasses. Thus the PDF technique has the potential to become a tool for structure determination that is highly needed in the newly emerging field of nanoscience and technology.

ACKNOWLEDGMENTS

The work was supported in part by NSF through Grant Nos. DMR 0304391 (NIRT) and DMR 0313963. The Advanced Photon Source is supported by the DOE under Contract No. W-31-109-Eng-38.

*Electronic address: petkov@phy.cmich.edu

[1] C. Sanchez, R. Morineao, and J. Livage, Phys. Status Solidi A **76**, 661 (1983).
[2] G. Micocci, A. Serra, A. Tepore, S. Capone, R. Rella, and P. Siciliano, J. Vac. Sci. Technol. A **15**, 34 (1997).
[3] J. Livage, Chem. Mater. **3**, 578 (1991).
[4] C. Julien, E. HaroPoniatowski, M. A. Camacho-Lopez, L. Escobar-Alarcon, and J. Jimenez-Jarquin, Mater. Sci. Eng., B **65**, 170 (1999).
[5] M. S. Whittingham, Electrochem. Soc. Proc. **99-24**, 7 (2000).
[6] S. Lutta, A. Dobley, K. Ngala, S. Yang, P. Y. Zavalij, and M. S. Whittingham, in 2001 Meeting Proceedings. Symposium V. *Nanophase and Nanocomposite Materials IV*, edited by S. Komarneni, J. C. Parker, R. A. Vaia, G. Q. (Max) Lu, and J.-I. Matsushita, MRS Symposia Proceedings No. 703 (Materials Research Society, Boston, 2002), p. V8.3.1.
[7] F. Zhang and M. S. Whittingham, Electrochem. Commun. **2**, 69 (2000).
[8] P. Zavalij and M. S. Whittingham, Acta Crystallogr., Sect. B: Struct. Sci. **55**, 627 (1999).
[9] G. Gu, M. Schmidt, P.-W. Chiu, A. Minett, J. Fraysse, G-T. Kim, S. Roth, M. Kozlov, E. Muñoz, and R. Baughman, Nature Mater. **2**, 316 (2003).
[10] J-F. Xu, R. Czerw, S. Webster, D. L. Carroll, J. Ballato, and R. Nesper, Appl. Phys. Lett. **81**, 1711 (2002).
[11] F. Krumeich, H.-J. Muhr, M. Niederberger, F. Bieri, B. Schnyder, and R. Nesper, J. Am. Chem. Soc. **121**, 8324 (1999).
[12] A. Dobley, K. Ngala, S. Yang, P. Zavalij, and M. S. Whittingham, Chem. Mater. **13**, 4382 (2001).
[13] L. Mai, W. Chen, Q. Xu, Q. Zhu, C. Han, and J. Peng, Solid State Commun. **126**, 541 (2003).
[14] J. M. Reinoso, H. J. Muhr, F. Krumeich, F. Bieri, and R. Nesper, Helv. Chim. Acta **83**, 1724 (2000).
[15] H. P. Klug and L. E. Alexander, in *X-ray Diffraction Procedures for Polycrystalline Materials* (Wiley, New York, 1974).
[16] V. Petkov, J. Appl. Crystallogr. **22**, 387 (1989).
[17] H. M. Rietveld, J. Appl. Crystallogr. **2**, 65 (1969).
[18] V. Petkov, S. J. L. Billinge, P. Larson, S. D. Mahanti, T. Vogt, K. K. Rangan, and M. G. Kanatzidis, Phys. Rev. B **65**, 092105 (2002).
[19] V. Petkov, P. N. Trikalitis, E. Bozin, S. J. L. Billinge, T. Vogt, and M. G. Kanatzidis, J. Am. Chem. Soc. **124**, 10 157 (2002).
[20] R. Wyckoff, *Crystal Structures* (Wiley, New York, 1964).
[21] Th. Proffen and S. J. L. Billinge, J. Appl. Crystallogr. **32**, 572 (1999).
[22] J. Galy and A. Carpy, Acta Crystallogr., Sect. B: Struct. Crystallogr. Cryst. Chem. **31**, 1794 (1975).
[23] P. Zavalij, F. Zhang, and M. S. Whittingham, Solid State Sci. **4**, 591 (2000).
[24] M. Worle, F. Krumeich, F. Bieri, M-H. Juhr, and R. Nesper, Z. Anorg. Allg. Chem. **628**, 2778 (2002).
[25] X. Wang, L. Liu, R. Bontchev, and A. J. Jacobson, Chem. Commun. (Cambridge) **9**, 1009 (1998).
[26] S. Iijima, Nature (London) **354**, 56 (1991).